General considerations on degradation of Solid Oxide Fuel Cell anodes and cathodes due to impurities in gases

Harumi Yokokawa [a,b,*], Katsuhiko Yamaji [a,1], M.E. Brito [a,1], Haruo Kishimoto [a,1], Teruhisa Horita [a,1]

[a] National Institute of Advanced Industrial Science and Technology (AIST), Energy Technology Research Institute, Higashi 1-1-1, Tsukuba, Ibaraki 305-8565, Japan
[b] Tokyo City University, Advanced Research Laboratory, Todoroki 8-15-1, Setagaya-ku, Tokyo 158-0082, Japan

ARTICLE INFO

ABSTRACT

The degradation mechanism of cathodes and anodes due to gaseous impurities has been considered to provide generalized understanding of materials behavior involved in degradation and hopefully to possible recovery processes. Considerations can be made in terms of (1) the chemical reactivity of gaseous impurities with a main component of electrode materials, (2) diffusivity of main components associated with chemical reactions, and (3) electrochemical reduction/oxidation processes of gaseous impurities in competing with recovery processes due to those electrochemical reactions or chemical reactions which lead to the volatilization of deposited substance and removal of poisons from the electrochemically active sites. The chemical reactivity of the main component with gaseous impurities can be well characterized in terms of the thermodynamic properties such as interaction parameters for intermetallic compounds or the stabilization energy/the valence stability of the transition-metal oxides for oxide electrodes. Diffusivity of main components should be discussed with the enhancement due to surface coverage of impurities. The electrochemical reduction/oxidation of the gaseous impurities provides the mechanism of impurities being deposited and accumulated at the electrochemical reaction sites. Possible recovery process could be examined by whether corresponding electrochemical or chemical process for the deposited substances to be volatilized is available.

© 2010 Elsevier B.V. All rights reserved.

1. Introduction

In recent years, there are growing strong interests in applying the solid oxide fuel cells to cogeneration systems for the residential houses [1]. Among the fundamental features of the SOFC systems as energy converters, the durability/reliability, in other words, life time is the most important in the early entry to the markets compared with the rest of the features, efficiency and cost, although the latter two features are also important and their achievement is closely related with the durability/reliability issues [2–10].

We have involved with the NEDO project on the reliability of SOFC stacks/modules conducted from 2005 to 2008 [3–5]. The main topic of this project was to make detailed analyses of cell components after a long term operation with the SIMS (Secondary Ion Mass Spectrometry) technique applied to the real SOFC stack materials. The following four stacks/modules were cooperated: segment

in series tubular cell made by Mitsubishi Heavy Industry (H1), Flatted tube cells made by Kyocera (L1), Seal-less tubular cell made by TOTO (H2), and Disk-type planar made by Mitsubishi Materials (L2). The following results were obtained [6]:

(1) It has been well recognized that the SIMS technique [5] can be successfully applied to detect the interdiffusion of elements across interfaces of cell components as well as detect the impurity migration within the SOFC stacks.
(2) Basically cation diffusion across the interfaces during operation is quite small. Exceptions are diffusion in cathode complex layers including ceria interlayers and diffusion in metals/alloys including oxide scales. In some cases, nickel sintering appears to be significant.
(3) Detected chromium deposited in the LSM cathode/YSZ-electrolyte interface is quite limited even though several per cent of performance degradation is observed. This suggests that in order to achieve a long life in the range of 40,000–90,000 h, it becomes essential to carefully control the accumulation of poisoning elements in the electrochemical reaction sites within the contamination level of 1–1000 ppm. For this region, only SIMS can be applied to detect the materials behavior.
(4) In some cases, contamination by impurities becomes significant. At the end of the project, it was not easy to find the

* Corresponding author at: National Institute of Advanced Industrial Science and Technology (AIST), Energy Technology Research Institute, Higashi 1-1-1, Tsukuba, Ibaraki 305-8565, Japan. Tel.: +81 29 861 4542/3 57063112;
fax: +81 29 861 4540/3 57063112.
E-mail addresses: h-yokokawa@aist.go.jp, h-yokoka@tcu.ac.jp (H. Yokokawa).
[1] Tel.: +81 29 861 4542; fax: +81 29 861 4540.

correlation of impurities and performance degradation which was in the range of 0.8–1.5%/1000 h.

These findings are quite important to improve the stack performance from 1%/1000 h level to 0.25 or 0.1%/1000 h. This also indicates further need to make more fundamental investigations on correlation between the degradation behavior and materials behaviors inside SOFC stacks.

Thus, a new NEDO project has been organized as five-year project from 2008 to 2013. One stack made by Tokyo gas/Kyocera joined newly to the NEDO project. Several university groups participate to clarify the degradation mechanism. There are several aims/strategies adopted in this project as given below:

(1) Various experimental facilities will be combined to observe the materials within stacks. In addition to SIMS, a new machine such as FIB/SEM will be introduced to obtain the microstructures of electrodes.
(2) Common approach: Universities/research institutes share the key concept that those electrochemical processes which are taken in fuel cells should be well described in terms of the local equilibrium approximation. This approximation is an old but fundamental idea for understanding the high temperature corrosion. Mizusaki et al. [11] proposed that the same idea can be well applied to the electrochemical process associated with cathode and anode electrode reaction mechanism. One of the merits of this approach is that understanding the interface chemistry is rather easy to be correlated with the electrochemical behavior; a most interesting example is the $La_2Zr_2O_7$ formation at the LSM/YSZ interface [12]. This can be also applied to sulphur poisoning.

The latter local equilibrium model seems to be powerful in obtaining the common degradation mechanism among various cathodes as well as nickel cermet anodes. In the degradation studies on cathodes, many reactions or elements have been tested. This can be interpreted in terms of thermodynamic stability relations [7,8]. For anodes, thermodynamic analyses have been made to clarify the chemical interaction between Ni and impurities. In recent years, a significant amount of efforts have been made in US to clarify the interactions between nickel and impurities originated from coal based fuels [10]. Since their results are quite interesting from the material chemical point of view with which our interpretation has been tested, attempts have been made to extract the important features from the respective poisoning phenomena, to combine those features to set up a common, well generalized model associated with degradation of electrode by foreign elements, and finally to apply new ideas/mechanism to respective poisoning system again, leading to new insight into the degradations.

2. Interpretation of PNNL/NETL/WVU results

Within the DOE/SECA project, PNNL (Pacific Northwest National Laboratory), NETL (National Energy Technology Laboratory) and WVU (West Virginia University) made intensive and extensive investigations on effects of coal-derived gaseous impurities on nickel-YSZ cermet anodes [10,13–19]. On the other hand, we have calculated and constructed the chemical potential diagrams for the Ni–M–O–H (M = S, Se, As, P) systems [20,21]; for the Ni–P–O–H system, we modified the early diagrams by adopting the thermodynamic data for the $HPO_n(g)$ ($n = 1,2,3$) as suggested by Bao et al. [22–24].
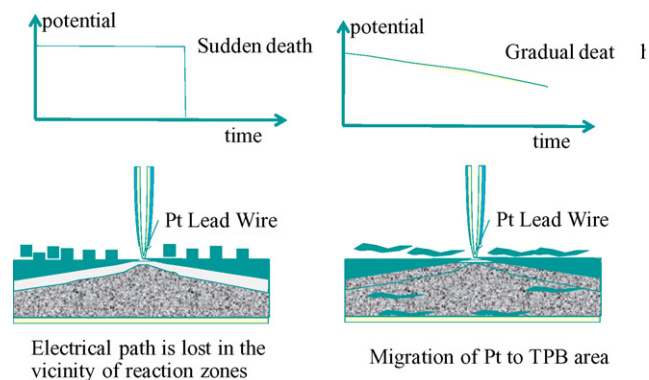

Fig. 1. Schematic comparison in electrical performance degradation between As and P in PNNL/NETL/WVU results [10,13–19].

2.1. Comparison between As and P

Both elements As and P show strong chemical affinity with nickel so that many intermetallic compounds are formed where nickel cermet anodes are encountered with such impurities. This is schematically illustrated in Fig. 1. Most interesting difference between two elements in degradation behavior is that As gives rise to a sudden death after no change in performance, whereas the performance degradation for the P case is observed from the beginning stage of contamination.

Fig. 2 collects the chemical potential diagrams in three different types. The first type is the Ellingham diagram for the M–O–H (M = As, P) systems. Gases in the H–O subsystem, namely, $H_2(g)$, $O_2(g)$, and $H_2O(g)$, are assumed at a pressure of 1 atm, whereas gaseous species containing M (As or P) are assumed at $p = 10^{-6}$ atm; this corresponds to 1 ppm contamination in fuels. The second type of diagram is the extended Ellingham diagram for the Ni–M–O–H (M = AS, P) systems which indicates the dominant chemical form of nickel in the presence of M or M compounds. When only Ni or NiO are given, this indicates that Ni is stable against such contaminants. The third type of diagram is the $\log a(M)$ vs. $\log p(O_2)$ plot at a selected temperature (1073 K). From the chemical potential diagrams, the followings can be derived (Fig. 2):

(1) Both elements exhibit strong tendency of forming nickel intermetallic compounds such as Ni_5As_2 or Ni_5P_2. This is one of common features.
(2) For gaseous species, there are big differences between two elements. Although the thermodynamic data for such gaseous species are not necessarily accumulated well, the following difference is important: In an anode atmosphere, As exists as As_4 or As_2 molecules rather than AsH_3, whereas P exists as PH_3 or HPO_2 when water vapor exist.
(3) The formation of oxysalts ($Ni_3(AsO_4)_2$ or $Ni_3(PO_4)_2$) is favored in the oxidative atmospheres.
(4) When interactions with nickel are considered, the above differences give rise to significant differences between two elements:
 (i) At 1 ppm contamination level, only the intermetallic compound formation is a dominant process for the As contamination, whereas the intermetallic formation, the oxysalt formation or the no interaction due to the HPO_2 formation are competitive depending on temperature and oxygen potential.
 (ii) With decreasing concentration, the HPO_2 formation becomes favored. Note however, the oxysalt formation remains as possible process.
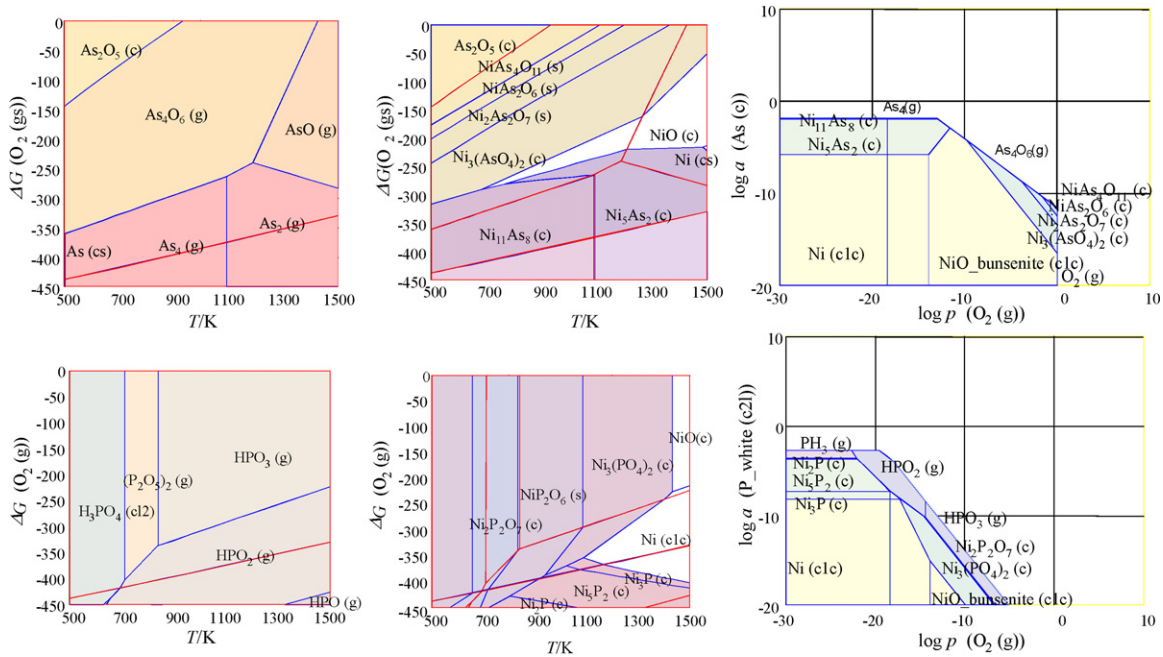
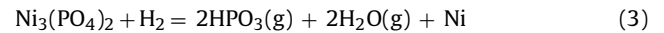**Fig. 2.** Comparison in chemical potential diagrams between Ni–As–O–H and Ni–P–O–H systems.

These thermodynamic features lead to the following interpretation for the experimental observations by PNNL/NETL/WVU as follows (see also Fig. 3):

(1) For the case of P contamination, PNNL/NETL/WVU found that P reaches to the YSZ-electrolyte and Ni/YSZ cermet interfaces. AIST also observed the concentration of P at TPBs by SIMS within the NEDO project. Those observed phosphors seem to directly attack electrochemically active sites. This can be written as two processes where vapors such as HPO_x play important roles.

$$PH_3(g) + 2H_2O(g) = HPO_2(g) + 3H_2(g) \quad (1)$$

$$3Ni + 2HPO_2(g) + 4O^{2-} = Ni_3(PO_4)_2 + 8e^- \quad (2)$$
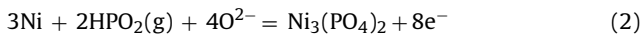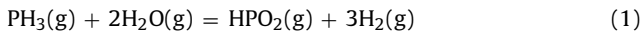
The second one is an electrochemically anodic reaction so that this is enhanced in the anode reaction sites. This is very reason why the performance degraded from the initial stage of contamination.

(2) No area of the $Ni_3(AsO_4)_2$ formation because of the oxygen potential mismatch. Even when As vapors reach to the TPBs, no poisoning effects appear. This is reason why no performance degradation was observed. On the other hand, Ni diffusion in Ni–As system is probably highly enhanced, leading to a sudden death. In the PNNL/NETL/WVU experiments, As did not reach to TPBs; this is probably due to strong ability of nickel to trap As containing vapors as intermetallic compounds.

(3) Compared with As, P can be penetrated through the reaction zone of intermetallic compound to the TPBs to form $Ni_3(PO_4)_2$.

(4) As recovery process for the P contamination, the volatilization reaction

$$Ni_3(PO_4)_2 + H_2 = 2HPO_3(g) + 2H_2O(g) + Ni \quad (3)$$

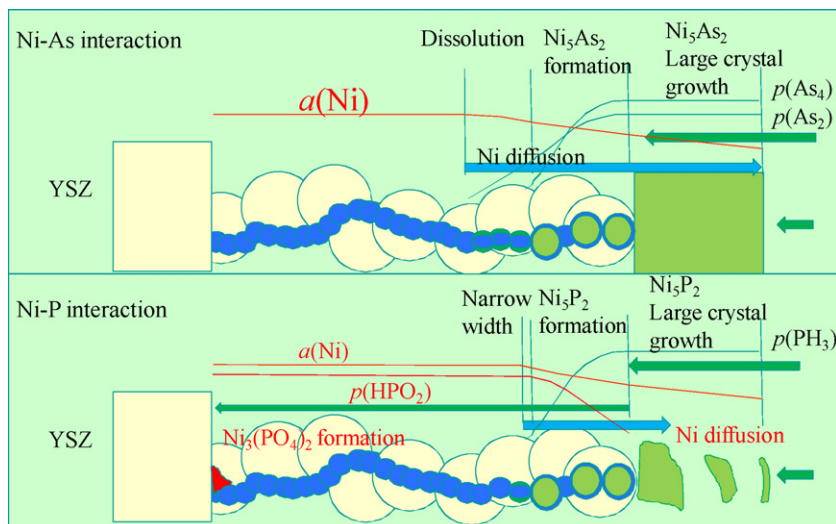can be considered. Note however that this is not the electrochemical reaction.

Fig. 3. Schematic view of mass transfer associated with poisoning associated with As and P.
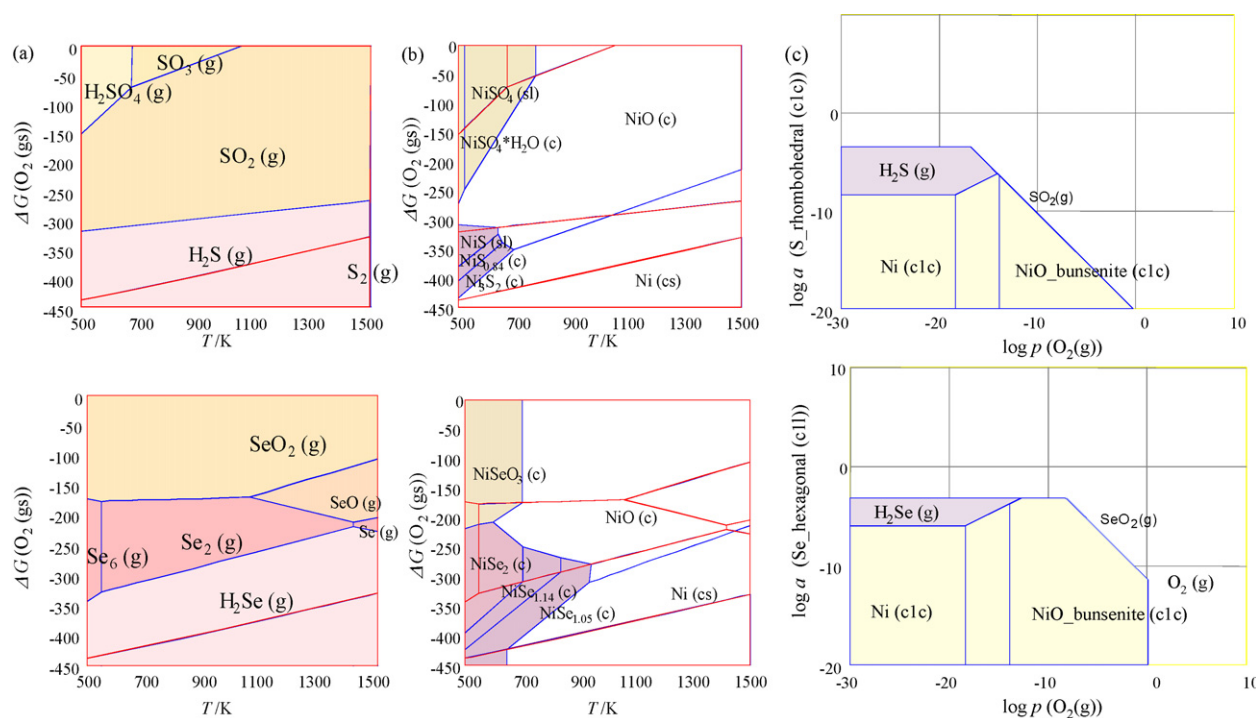
Fig. 4. Comparison in chemical potential diagrams between S and Se. (a) Ellingham diagrams for the M–O–H (M = S, Se) systems, (b) extended Ellingham diagrams for the Ni–M–O–H (M = S, Se) systems and (c) log a(M) vs. log p(O_2) plot at 1073 K. Partial pressure of M-containing gases is assumed to be 10^{-6} atm.

From this comparison, important factors to be considered for the nickel–impurity interactions can be extracted as follows:

(1) Trap rate: when impurities are reacted with nickel, the trap rate at the entrance becomes important. If this is nearly 100%, essentially no gaseous species reach to the electrochemical sites. This suggests that performance degradation may be only due to deterioration in gaseous channel or electrical path within the anode layer.
(2) Availability of deposition reactions: for gaseous impurities to act as poisons for electrochemical reactions, such gases have to be adsorbed or deposited in the vicinity of the electrochemical reaction sites.
(3) Availability of electrochemically assisted deposition reaction: if the deposition reaction proceeds as electrochemical reaction, this should be enhanced. For this purpose, the gaseous species has to be interacted with electrochemically active species such as oxide ions.

2.2. Comparison between S and Se

PNNL/NETL/WVU obtained interesting results on poisoning due to S and Se. Most interesting points are the followings:

(1) The reaction of Ni with Se results in the formation of NiSe in the interface between the YSZ-electrolyte and the Ni cermet anodes. This is essentially the same behavior as the Ni–S interaction when the NiS formation occurs for the higher concentration cases.
(2) The initial behavior is similar in a sense that the electrical potential decreases immediately after the impurity gases are introduced and then becomes constant.
(3) The main difference appears in the recovery process after the fuel is switched back to non-poison fuels. For the H_2S case, a slow recovery process is observed, whereas no recovery can be seen for the H_2Se case.

The difference in the recovery process is quite interesting from the thermodynamic point of view which is summarized as the chemical potential diagrams given in Fig. 4. Comparison between the S–O–H and the Se–O–H systems indicates that significant different features can be in the dominant species in the anode atmosphere. For the case of the S–O–H system at the partial pressure of 10^{-6} atm for the S-containing species, H_2S is stable in the hydrogen dominant area and SO_2 can be dominant in the oxidative side of the H_2O-dominant area. For the Se–O–H system, H_2Se is similarly stable in the hydrogen dominant area, whereas the Se_2 dominant area appears between the SeO_2 dominant are and the H_2Se dominant area for the H_2O-dominant area. This difference should be related with the difference in the recovery process.

From the chemical potential diagrams for the Ni–M–O–H (M = S, Se) systems, it is clear that the interaction between Ni and S or Se is week compared with those with As or P. This corresponds well to the fact that the formation of Ni–M (S, Se) intermetallic compounds does not occur at the entrance area where the impurities encounter with Ni first. As shown in the log a(M) vs. log p(O_2) plot, there is an interesting feature in the thermodynamic property for the interaction of Ni and S or Se in the anode atmosphere; that is, with increasing oxygen potential in the anode atmosphere of H_2/H_2O mixture, the activity of M(S/Se) increases under the condition of a constant partial pressure of 10^{-6} atm for H_2Se. This is the reason why NiS or NiSe are formed at the interface between the YSZ-electrolyte and the nickel cermet anodes, if any. Typical situation is illustrated schematically in Fig. 5.

3. Generalization of important processes associated with impurity poisoning effects

From the above discussions in addition to the accumulated knowledge on the poisoning effects [7–9], we can extract several important factors to be considered in the impurity poisoning effects (see Fig. 6).
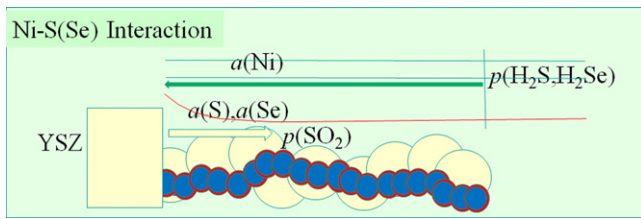
Fig. 5. Schematic view of mass transfer associated with poisoning associated with S and Se.
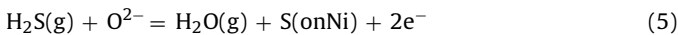
3.1. Compound formation

One component of electrode constituents can react with impurities to form a new compound. In this case, gaseous impurities are always carried with the gaseous flow. Thus, the availability of the diffusion path for the component to be reacted becomes important. For the case of nickel cermet anodes, the diffusivity of nickel becomes crucial in determining the morphological feature of the formed compounds. For the case of NI_5As_2 or Ni_5P_2, those compounds are formed against the gaseous flow, indicating that the supplies of nickel to the reaction front are sufficiently high and fast enough; this is probably because the nickel diffusion is enhanced in the presence of adsorbed species which can have the strong interaction with nickel. The sudden death in the As impurity case should be resulted from this fast diffusion of nickel, leading to cut off the electrical percolation path (Fig. 3).

### 3.2. Electrochemical side reactions involved with the impurities

Impurity containing gases can reach the electrochemically active sites and can be electrochemically oxidized or reduced in a similar manner to the main electrochemical reaction. Most typical reaction is the chromium poisoning. This reaction can be written as

$$2CrO_3(g) + 6e^- = Cr_2O_3 + 3O^{2-} \tag{4}$$

Similarly sulphur poisoning can be written as

$$H_2S(g) + O^{2-} = H_2O(g) + S(onNi) + 2e^- \tag{5}$$

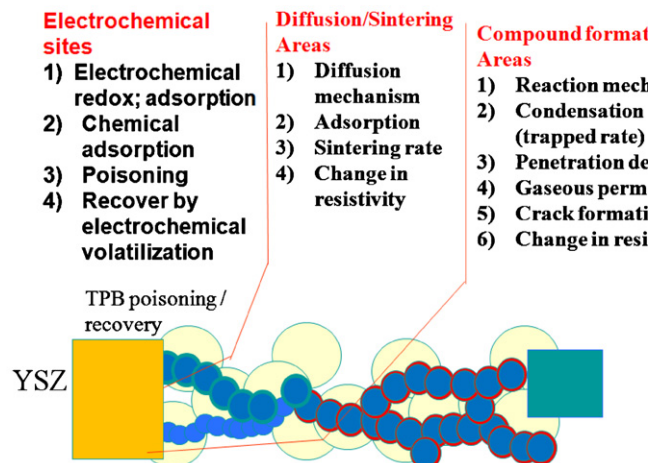**Fig. 6.** Generalization of respective processes involved in the poisoning effects by foreign impurities in gases.

The present results suggest that the recovery process can be also electrochemical reaction: for the case of Cr poisoning, we observed curious behavior that the Cr deposited amount is smaller when the applied voltage was increased for LSM–GDC system. Although there are many things to be considered on these results, this fact suggests that there must be one reaction mechanism in which deposited Cr_2O_3 will be volatilized again or another mechanism in which deposition of Cr_2O_3 is hindered. This seems to be the following reaction:

$$Cr_2O_3 + O_2(g) + 2H^+ + 2e^- = 2CrO_2(OH)_2(g) \tag{6}$$
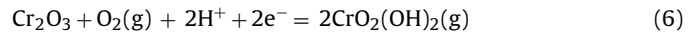
This reaction can be rewritten as a combination of the following two reactions:

$$0.5O_2(g) + 2H^+ + 2e^- = H_2O(g) \tag{7}$$

$$Cr_2O_3 + 1.5O_2(g) + H_2O(g) = 2CrO_2(OH)_2(g) \tag{8}$$
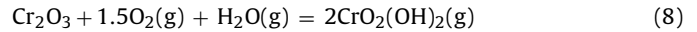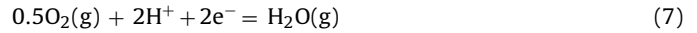
The first one is the cathodic reaction to form water vapors, whereas the second one is the volatilization reaction of Cr_2O_3 with oxygen gas as well as water vapor to form $CrO_2(OH)_2$.

Although proton is quite miner species in the YSZ, we can expect some contribution of protons to the electrochemical side processes associated with doped ceria [25–29]. In the present study described above, we suggested the following:

$$S(onNi) + 2O^{2-} = SO_2(g) + 4e^- \tag{9}$$

From these two examples, we can see the important feature of the electrochemical reactions involved with the impurities gases; that is, condensation and volatilization reactions are not the microscopically reversible reaction in a sense that the major species involved in the main electrochemical reactions are always the same between the deposition reaction and the volatilization reaction. In view of this, normal microscopic reversibility does not hold.

3.3. Sintering behavior

One of the main degradation processes of the Ni cermet anodes is sintering. When operational temperature is high around 900–1000 °C, sintering takes place in a slow speed in a range of several 1000 h. When the operational temperature decreases down to 800 °C, curiously enough, sintering of nickel appears more frequently than at 1000 °C. This is probably because of impurities which tend to absorb or dissolute at lower temperatures. Typical contaminant will be sulphur and phosphor. Such sintering phenomena will be discussed in terms of change in diffusion properties as well as the surface energy changed by the adsorption.

4. Applications of generalized models to respective effects

After establishing the generalized model, it becomes rather easy to construct possible whole features of one particular impurity effect. For example, we can consider the chromium poisoning on those cathodes materials based on lanthanum strontium ferrites or cobaltites.

(1) $SrCrO_4$ formation can be easily detected in normal post-test examinations. Even so, the $SrCrO_4$ formation alone does not lead to the degradation of electrode performance.
(2) Careful examination is needed on chromium deposition in the electrochemically active sites, namely, in the bottom area of the cathode layer. The amount of chromium deposited around this area is determined by two effects; one is the trapping rate of chromium containing gases at the entrance areas, the other being the reaction rate of escaped gasses in a deposition area.
(3) The deposition rate will depend on the layer structure of cathode and doped ceria interlayer. Since this combination is not

thermodynamically stable and some reactions can proceed, there are basically two reactions with chromium containing vapors; one is the reaction with cathode itself, the other being the reaction with the dopant in the ceria layer to form rare earth chromite. Usually, the rare earth chromites are electron conductive so that harmful effects will be small. Even so, among the transition-metal perovskite oxides, chromites exhibit less active in surface exchange, leading some lowering in the electrode activity [8].

For the LSM cathode, we can add the following cases where rare earth doped ceria are used instead of YSZ;

(1) The rare earth dopant in ceria can react with chromium vapor to form the rare earth chromites. This reaction can be taken place as electrochemical reaction or as normal chemical reaction.
(2) Since protons can be available in a more significant amount in doped ceria than YSZ, Eq. (6) can be feasible for LSM/doped ceria combination. This can give some explanation for the experimental observation by Matsuzaki and Yasuda [30] which showed some difference between LSM/YSZ and LSM/SDC in chromium poisoning.
(3) In our own experiments, some curious features were observed that the deposited amount of chromium on LSM/GDC interface is smaller for 0.5 V polarization compared with 0.3 V polarization. Although large polarization may change the cathode reaction mechanism to extend the reaction zone, we can expect that the electrochemical volatilization reaction proceeds more significantly when the polarization is increased.

By summarizing these features, we can say that the features of reactions between the cathode and the chromium vapor are complicated as suggested from the thermodynamic calculations as well as predicted complicated nature of kinetics involved. This explains why many investigations exhibit quite different features for chromium poisoning.

At present, we have the following understanding about how to clarify the chromium poisoning;

(1) SIMS technique: In order to detect the poisoning element at the electrochemically active sites corresponding to the degradation rate of 1%/1000 h, SIMS is only one method available.
(2) Analyses on chemical state of impurities in TPBs: In order to correlate the accumulated amount of impurities and the performance degradation, it is essential to identify the chemical form of impurities and their physical properties associated with the electrode activity. Even so, at present it is not easy to identify the chemical state except for the case where detailed examinations by TEM will be succeeded in finding the very compound. Instead, the thermodynamic analyses will be alternative way of predicting the chemical form and its physical properties.

5. Summary

The generalized model for the reaction of electrode components with gaseous impurities has been successfully established on the basis of the accumulated poisoning effects for cathodes as well as anodes. When the generalized model is applied to a specific impurity effect, we have to treat complicated features involved. Even

so, this provides a reasonable basis of understanding the observed complicated features of poisoning phenomena.

References

[1] M. Suzuki, S. Iwata, K. HIgaki, S. Inoue, T. Shigehisa, I. Miyachi, H. Nakabayashi, K. Simazu, ECS Trans. 25 (2) (2009) 143–148.
[2] H. Yokokawa, in: W. Vielstich, H. Yokokawa, H.A. Gasteiger (Eds.), Handbook of Fuel Cells Fundamentals Technology and Application, vol. 6. Advances in Electrocatalyst, Materials, Diagnostics, and Durability, John Wiley & Sons, 2009, pp. 923–932.
[3] H. Yokokawa, N. Sakai, T. Horita, K. Yamaji, in: W. Vielstich, H. Yokokawa, H.A. Gasteiger (Eds.), Handbook of Fuel Cells Fundamentals Technology and Application, vol. 6, Advances in Electrocatalyst, Materials, Diagnostics, and Durability, John Wiley & Sons, 2009, pp. 979–991.
[4] H. Yokokawa, T. Horita, K. Yamaji, H. Kishimoto, Y.P. Xiong, M.E. Brito, Proc. 8th European Solid Oxide Fuel Cell Forum, B1004, July, 2008.
[5] K. Yamaji, N. Sakai, H. Kishimoto, T. Horita, M.E. Brito, H. Yokokawa, in: W. Vielstich, H. Yokokawa, H.A. Gasteiger (Eds.), Handbook of Fuel Cells Fundamentals Technology and Application, vol. 5, Advances in Electrocatalyst, Materials, Diagnostics, and Durability, John Wiley & Sons, 2009, pp. 555–565.
[6] H. Yokokawa, T. Horita, K. Yamaji, H. Kishimoto, M.E. Brito, J. Korean Ceram. Soc. 47 (1) (2010) 26–38.
[7] H. Yokokawa, T. Horita, N. Sakai, J. Yamaji, M.E. Brito, Y.P. Xiong, H. Kishimoto, Solid State Ionics 177 (2006) 3193–3198.
[8] H. Yokokawa, H. Sakai, T. Horita, K. Yamaji, M.E. Brito, H. Kishimoto, J. Alloy Compd. 452 (2008) 41–47.
[9] H. Yokokawa, H. Tu, B. Iwanschitz, A. Mai, J. Power Sources 182 (2008) 400–412.
[10] O.A. Marina, L.R. Pederson, A. Martinez, R. Gemmen, K. Gerdes, H. Finklea, I.B. Celik, Presented in Fuel Cell Seminar 2009 and their related work, 2009.
[11] J. Mizusaki, H. Tagawa, K. Tsuneyoshi, A. Sawata, J. Electrochem. Soc. 138 (1991) 1867.
[12] H. Yokokawa, Annu. Rev. Mater. Res. 33 (2003) 581–610.
[13] J.P. Trembly, A.I. Marques, T.R. Ohrn, D.J. Bayless, J. Power Sources 158 (2006) 263–273.
[14] A.I. Marques, T.R. Ohrn, J.P. Trembly, D.C. Ingram, D.J. Bayless, J. Power Sources 164 (2007) 659–667.
[15] R.S. Gemmen, J. Trembly, J. Power Sources 161 (2006) 1084–1095.
[16] J.P. Trembly, R.S. Gemmen, D.J. Bayless, J. Power Sources 163 (2007) 986–996.
[17] J.P. Trembly, R.S. Gemmen, D.J. Bayless, J. Power Sources 169 (2007) 347–354.
[18] J.P. Trembly, R.S. Gemmen, D.J. Bayless, J. Power Sources 171 (2007) 818–825.
[19] B. Xu, J.W. Zondlo, H.O. Finklea, O. Demircan, M. Gong, X.B. Liu, J. Power Sources 193 (2009) 739–746.
[20] H. Yokokawa, H. Kishimoto, K. Yamaji, T. Horita, J. Electrochem. Soc. 157 (6) (2010).
[21] H. Yokokawa, H. Kishimoto, K. Yamaji, T. Horita, ECS Trans. 25 (2) (2009) 2131–2140.
[22] J. Bao, G.N. Krishnan, P. Jayaweera, J. Perez-Mariano, A. Sanjurjo, J. Power Sources 193 (2009) 607–616.
[23] J. Bao, G.N. Krishnan, P. Jayaweera, K.H. Kau, A. Sanjurjo, J. Power Sources 193 (2009) 617–624.
[24] J. Bao, G.N. Krishnan, P. Jayaweera, A. Sanjurojo, J. Power Sources 195 (5) (2010) 1316–1324.
[25] H. Kishimoto, N. Sakai, K. Yamaji, T. Horita, M.E. Brito, H. Yokokawa, ECS Trans. 13 (26) (2008) 105–114.
[26] T. Horita, H. Kishimoto, K. Yamaji, N. Sakai, Y.P. Xiong, M.E. Brito, H. Yokokawa, Solid State Ionics 177 (2006) 3179–3185.
[27] T. Horita, H. Kishimoto, K. Yamaji, N. Sakai, Y.P. Xiong, M.E. Brito, H. Yokokawa, Adv. Sci. Technol. 45 (2006) 1857–1863.
[28] H. Yokokawa, T. Horita, N. Sakai, K. Yamaji, M.E. Brito, Y.P. Xiong, H. Kishimoto, Solid State Ionics 177 (2006) 1705–1714.
[29] H. Yokokawa, T. Horita, N. Sakai, K. Yamaji, M.E. Brito, Y.P. Xiong, H. Kishimoto, Solid State Ionics 174 (2004) 205–221.
[30] Y. Matsuzaki, I. Yasuda, J. Electrochem. Soc. 148 (2001) A126.